Joint Swapping and Purification with Failures for Entanglement Distribution in Quantum Networks

***Abstract*—Swapping and purification are the two fundamental building blocks for multi-hop quantum networks. However, their interplay and its impact on end-to-end fidelity and cost are not yet fully explored. Existing scheduling algorithms address this problem under certain simplified assumptions and models that may not fully capture the complexities of real scenarios. In this work, we first consider more general assumptions that account for operation failures and extend a tree-based modeling approach for joint swapping and purification. Then, for the first time, we analytically prove the previous conjecture that the optimal strategy under *Binary system* is always to purify the entanglements before any swapping. This sheds light on the protocol and device design for entanglement distribution in quantum networks. We then further propose a tree-based algorithm, which can efficiently schedule swapping and purification along a path for both *Binary* and *Werner systems*. Extensive simulations have been conducted to evaluate the proposed method against the existing solutions, and the results show that our method uses fewer entanglements to establish qualified end-to-end entanglements and thus achieves higher network throughput.**

***Index Terms*—Quantum Swapping, Quantum Purification, Fidelity, Entanglement Distribution, Quantum Network.**

I. Introduction

In a quantum network [1]–[4], a pair of entangled particles (EPR pairs) needs to be distributed to the source and destination nodes (denoted as a Source-Destination (SD) pair) so that quantum bits/status can be transferred between them via teleportation. Such entanglements are the key resource in quantum networks [5]–[8]. However, establishing long-distance (multi-hop) entanglements is a challenging task. Unlike in classic networks, we cannot simply copy the state of one particle due to the no-cloning principle of quantum states. Simply sending photons (the usual particle used to carry quantum information) in optical fibers far away is also infeasible because photons decay exponentially as they travel in fibers.

Entanglements in quantum networks are initially generated over short quantum links (usually optical fibers). One link may contain multiple channels to generate entanglements on the two endpoints of the link. Such link-level entanglements can be later connected by the swapping operation to form long-distance connections. *Quantum swapping* takes two adjacent entanglements as inputs and generates a longer entanglement. This operation can be repeated over a path until we obtain an end-to-end (E2E) entanglement on the desired SD pair. However, while swapping establishes a longer entanglement, it also decreases the quality of the entanglement (measured by *fidelity*). Then, *quantum purification* is introduced in quantum networks: by sacrificing additional entanglements on the same two nodes, we can improve the fidelity of the entanglement.

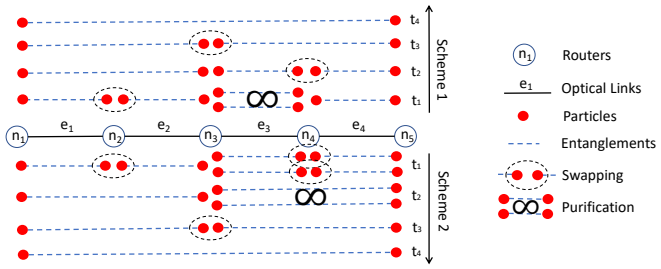

Fig. 1. Swapping and purification schemes (SPS): two example schemes along a path of four quantum links.

In short, swapping extends the distance of entanglements at the price of their fidelity; while purification improves fidelity by consuming additional entanglement(s). Combining these two basic operations, we can build long-distance (multi-hop) entanglements with high fidelity.

As shown in Fig. 1, we now consider an example of a quantum path from node n_1 to n_5 connected by four optical links, which generate entangled particle pairs as entanglements. Fig. 1 shows two possible sequences of swapping and purification operations (schemes) to establish the E2E entanglement between n_1 and n_5. In Scheme 1, at t_1, links e_1 and e_2 generate one entangled pair, separately. Because each pair has one particle on router n_2, swapping can be performed by n_2 to obtain an entanglement between n_1 and n_3 (at t_2). At the same time, link e_3 generates two entanglements, which share the same end nodes (n_3 and n_4), at t_1. Thus, a purification can be performed collaboratively by n_3 and n_4. If it succeeds, an entanglement of higher fidelity is established on link e_3. Via more swappings, Scheme 1 establishes an E2E entanglement between n_1 and n_5 at t_4. Scheme 2 gives an E2E entanglement on the same ends via a different swapping and purification order. Note that classic communications parts of those operations are ignored in this paper, and t_i's are not real-time stamps but only for marking the order of operations.

How swapping and purification interfere with each other, i.e., scheduling the swapping and purification operations to reach a specific final E2E fidelity with the least number of entanglements consumed, is still one open challenge in quantum networks. As shown in the example of Fig. 1, to acquire one entanglement for an SD pair connected by a quantum path, different *Swapping and Purification Schemes* (SPS) [9], [10] can be applied. Two extreme types of SPS solutions are (i) *PS scheme:* purify the entanglements immediately after their generation on each link, then swap links to establish the E2E entanglement; (ii) *SP scheme:* firstly generate massive low-

quality E2E entanglements by swapping and then perform purification over them. Obviously, you can also have a hybrid scheme that purifies intermediate entanglements after some swappings but before they are end-to-end. In Fig. 1, Scheme 1 follows the PS scheme, while Scheme 2 is a hybrid scheme.

A few studies have explored joint scheduling of swapping and purification but within a relatively limited scope. Some works [10]–[13] directly adopt one of the schemes without detailed justification, while others [14] provide only limited empirical study. Until recently, some analyses [15]–[17] have theoretically studied joint swapping and purification schemes but based on impractical assumptions, such as the absence of operation failures. To the best of our knowledge, no existing work has comprehensively analyzed the optimal SPS solutions (e.g., PS/SP/hybrid) while accounting for operation failures. This remains an important open problem as the optimal SPS is critical for device and protocol design for quantum networks. For example, if PS is indeed the best one, we may consider embedding purification into the link level (to allow fast purification over optical fibers) and design the repeaters accordingly. If not, we may need to consider collaboration between non-adjacent routers, which can be much more complicated.

In this paper, we fully explore the joint SPS problem. We first generalize the assumptions (by considering arbitrary operation orders and possible swapping/purification failures) and formulate an *Optimal Swapping and Purification Scheme* (OSPS) problem. By absorbing purification into the current tree-based modeling, we introduce the concept of *Swapping and Purification Tree* (SPT) to represent and analyze any possible solution of OSPS. We also propose a dynamic programming based SPS method, which enhances our understanding of the structure of SPS problem. These provide the foundation of our further analysis and solutions. By using the SPT model, we formally prove that the optimal solution of OSPS under *Binary system* follows the PS scheme. Furthermore, we propose a new tree-based solution, which works under both *Binary* and *Werner systems*. Via extensive simulations, we confirm our proposed method outperforms state-of-the-art solutions with both noisy and noiseless gates (with noisy channels). Overall, our contributions in this paper are three-fold.

1) We present a new modeling method for joint SPS in Section III, by considering the impact of operational failures. We then formally introduce the optimal SPS problem which aims to minimize the expected cost while achieving required E2E fidelity.
2) We prove that the optimal SPS solution under Binary systems follows the PS scheme (i.e., performing purification before swapping) in Section IV. To the best of our knowledge, this is the first formal theoretical analysis with operation failures on the SPS problem.
3) We propose a new branching tree method for SPS problem in Section V, which is able to handle joint (hybrid) optimization of swapping and purification. Our simulation results in Section VI then confirm that it outperforms the state-of-the-art solutions under both Binary and Werner systems.

II. Related Works

Entanglement Distribution and Routing. Early works on entanglement distribution focus on maximizing network throughput or minimizing delay without considering fidelity and purification. For example, ORED [12] models throughput maximization as a linear programming problem, while [18] proposes an opportunistic routing to reduce the delay. [19] has more specific assumptions on entanglement generation on optical links and uses predetermined paths between SD pairs for routing. FENDI [20] adopts the ORED framework and considers fidelity but not purification, improving fidelity and delay by reducing path length. Yang *et al.* [21] propose an online routing algorithm to enhance efficiency and scalability. These fidelity-agnostic algorithms often result in low-fidelity E2E entanglements, especially as the hop number increases.

Connection Quality Enhancement. Improving E2E entanglement fidelity can be attempted through purification over multiple E2E entanglements (as an SP scheme), though it is less effective for low-fidelity E2E entanglements. To overcome this, Zhao *et al.* [10] and Li *et al.* [11] both design greedy algorithms to keep finding the critical link (with either the largest gradient or the most fidelity increase after purification) and purifying it until the E2E fidelity threshold is met. Such methods use the PS scheme, but their calculation of expected sacrificial entanglements is greatly simplified (and the results are limited, e.g., both their solutions do not work under the Werner system). Jia and Chen also study joint swapping and purification in their recent series [15]–[17]. Their latest work [17] is able to find near-optimal paths between SD pairs and performs path selection to maximize overall throughput. However, their optimality is defined on additive pseudo metrics (not the real fidelity and throughput) and they assume no operation failures. Victoria *et. al* [22] propose a hybrid method that purifies after a certain fixed number of swappings. Jiang *et. al* [23] optimizes the total operation time via a dynamic programming based approach. All the works above ignore swap/purification failures. Instead, our tree-based solution is able to handle both failures of swapping/purification and complicated hybrid schemes.

Modeling and Analysis. Modeling E2E entanglement with hybrid swapping and purification is complex. Some works, like [12], [24], use tree structures for modeling swappings along quantum paths but do not include purification. Incorporating purification into the tree is easy as it also has two inputs and one output, but it is hard to perfectly absorb its properties. For example, the probability of purification failure is related to the fidelity of input pairs. When the tree is larger, how to compute the fidelity and expected entanglements used by this tree becomes challenging. Chang *et al.* [25] noticed that the associativity of operators helps to analyze the throughput on a single path, but does not consider fidelity. In this work, we use associativity to explain some properties of SPS. Jia and Chen [15]–[17] present the first closed-form fidelity of multiple purifications and optimal SPS for Werner systems. However, their analysis assumes no operation failure and narrowed hardware parameters, which limits its application. Instead,

our analysis focuses on Binary system, considers operation failures, and allows more flexible hardware parameters.

III. Quantum Background and SPS Modeling

A. Quantum States and Noise

A quantum bit can be in a superposition of multiple states, e.g., two states in a 2-state system. Such states can be expressed by $|\psi\rangle = \alpha|0\rangle + \beta|1\rangle$, where α and β are complex numbers. This formula describes a state $|\psi\rangle$ that, upon measurement, turned to be $|0\rangle$ with probability $|\alpha|^2$, and to be $|1\rangle$ with probability $|\beta|^2$, where $|\alpha|^2 + |\beta|^2 = 1$. Similarly, when two qubits are entangled (called ebits), we are interested in the mixture of the four states,

$$|\psi\rangle = \alpha_{00}|00\rangle + \alpha_{01}|01\rangle + \alpha_{10}|10\rangle + \alpha_{11}|11\rangle. \quad (1)$$

The squared coefficients still indicate the probability of the results and they sum to 1, e.g., we may get $|00\rangle$ with probability $|\alpha_{00}|^2$. Especially, the four special Bell states (also, interchangeably in this paper, EPR pairs) are: $|\Phi^{\pm}\rangle = \frac{1}{\sqrt{2}}(|00\rangle \pm |11\rangle)$ and $|\Psi^{\pm}\rangle = \frac{1}{\sqrt{2}}(|01\rangle \pm |10\rangle)$. We can express a pair of ebits not only by (1), but also by the Bell states:

$$\begin{aligned}\rho =& F_1 \left|\Phi^+\right\rangle\left\langle\Phi^+\right| + F_2 \left|\Psi^-\right\rangle\left\langle\Psi^-\right| \\ &+ F_3 \left|\Psi^+\right\rangle\left\langle\Psi^+\right| + F_4 \left|\Phi^-\right\rangle\left\langle\Phi^-\right|, \end{aligned} \quad (2)$$

where $\sum_i F_i = 1$. Note that ρ is not a vector like $|\psi\rangle$ in (1) but a matrix, and F_i's are the diagonal elements. Typically, we hope ρ to be a pure state of one of the four Bell states, e.g., without loss of generality, $|\Phi^+\rangle$. Then, the **fidelity** of an EPR pair is $F = F_1$, which means the probability that the EPR pair is in the desired state. In perfect systems, we have $F = 1$. In reality, however, the entanglements are always noisy, so we only have $F < 1$, and the other non-zero diagonals indicate the probability of being in the undesired states.

Quantum States. In this paper, we consider two formats of Eq. (2). For the *Binary state* [13], we define fidelity $F = F_1$ and allow only one of F_2, F_3, F_4 to be non-zero (i.e, $(1-F)$). E.g., in [13], $F_3 = 1 - F$. We are interested in such a state because it allows faster purification [13]. The other format is the *Werner state*, usually associated with the worst case noise: the entanglement is i) totally destroyed with probability p, or ii) left untouched with probability $1-p$. Such noisy channels are also known as depolarizing channels. The result density matrix is $\rho = (1-p)|\Phi^+\rangle\langle\Phi^+| + p \cdot \frac{1}{4}I$, where I is the identity matrix and $\frac{1}{4}I$ represents the totally destroyed entanglement.

Noise Models. We consider noise introduced in two stages: entanglement generation and quantum operations (i.e., swapping and purification). We consider two settings of state representations and noise: (1) Binary states with noisy entanglement generation and noiseless quantum operations; ii) Werner states with noisy entanglement generation and noisy quantum operations. We are interested in those two settings because the first setting allows faster purification protocols, while the second one represents the general (worst case) noise model. More details about those two settings and protocols will be discussed in the next part of this section. In the rest of this paper, we refer to those two settings by **Binary and Werner systems**. In other papers, the Binary/Werner states are sometimes called dephased/depolarized states, respectively.

B. Swapping and Purification

Now, we look at the two fundamental building blocks: *swapping* and *purification*, and briefly describe how they are conducted. For more details, please refer to [10].

Swapping. Swapping, or more generally, teleportation, involves sending a quantum state to a remote node with the help of an EPR pair. When the qubit to be teleported is already entangled with another qubit, we call it a swapping: two entanglements are connected into a longer one. The density matrix of the output entanglement can be expressed by the diagonals of the two input states. A detailed calculation is given by formula (10.9) in [26]. In this paper, we are only interested in the output fidelity (the first diagonal element), $F_1^{out} = \sum_i F_i^1 F_i^2$, where F_i^1/F_i^2 are the diagonals of the first/second input pair. It is easy to see that the output fidelity is the probability that the two input pairs are in the same states, no matter in the desired one ($F_1^1 F_1^2$) or not ($\sum_{i=2,3,4} F_i^1 F_i^2$). The formula in [26] gives us the most general case as it allows all diagonals to be independent. When bringing the constraints of those terms in Binary/Werner states, we obtain their swapping functions S_b (in Binary systems) and S_w (in Werner systems). Suppose the fidelity of the two input entangled pairs is f_1 and f_2, separately; then the fidelity of the output pair can be modeled as follows

$$S_b(f_1, f_2) = f_1 f_2 + (1-f_1)(1-f_2), \quad (3)$$

$$S_w(f_1, f_2) = f_1 f_2 + \frac{1}{3}(1-f_1)(1-f_2). \quad (4)$$

Note that the *success probability of swapping* does not rely on the input fidelity, but its implementation (e.g., 0.5 for linear optics, 0.625 [27] or 0.75 [28] for improved ones, and 1.0 for deterministic BSM [29]). We allow it in $(0.5, 1)$ in this paper.

Purification. We consider the two most popular and well-studied purification protocols: BEJMPS [13], [30] and BBPSSW [31]. DEJMPS is efficient in terms of improving the output fidelity when two input pairs are in the Binary state, while BBPSSW requires the input states in Werner state (usually associated with the worst-case noise). This is also the reason why we consider Binary/Werner systems. Note that the output of BBPSSW may not be in the Werner state, but we can easily bring it back by depolarization [31] [32].

Purification consists of two CNOT gates and a Bell state measurement (BSM). The two CNOT operations are conducted by using one of the input pairs as control qubits, the other pair as the target qubits. When the BSM result on the target pair agrees (i.e., the two qubits are in the same state), the purification succeeds and the other input pair is left with higher fidelity. Otherwise, it fails and both pairs are discarded without any outcome. Such inevitable failures are exactly one of the major reasons why it is not easy to find a good SPS. By the definition of the two purification protocols, the fidelity of their output pairs can be modeled as

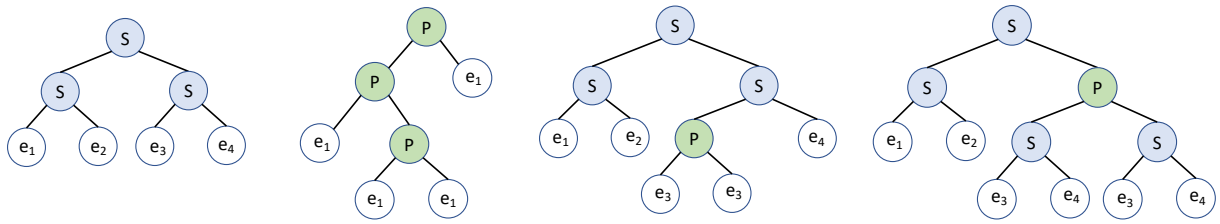

(a) ST for Scheme 1/2 (b) PT for link e_1 (c) SPT for Scheme 1 (d) SPT for Scheme 2

Fig. 2. Modeling of different trees: (a) the swapping tree (ST) of Scheme 1 and 2 (ignoring purification); (b) an example purification tree (PT) over link e_1; (c)/(d) the swapping and purification tree (SPT) of Scheme 1/2.

$$P_b(f_1, f_2) = \frac{f_1 f_2}{f_1 f_2 + (1-f_1)(1-f_2)} = \frac{f_1 f_2}{f_1 f_2 + \bar{f}_1 \bar{f}_2}, \quad (5)$$

$$P_w(f_1, f_2) = \frac{f_1 f_2 + \frac{1}{9}\bar{f}_1 \bar{f}_2}{f_1 f_2 + \frac{1}{3}[f_1 \bar{f}_2 + \bar{f}_1 f_2] + \frac{5}{9}\bar{f}_1 \bar{f}_2}, \quad (6)$$

where $\bar{f}_i = 1 - f_i$. The denominators in these formulas are the probability that the result of BSM agrees, which is exactly the *success probability of purification*. The numerators are the first diagonals obtained from the protocols, respectively. For example, in Binary systems, the success probability is when both pairs are in the desired state $(f_1 f_2)$ or both not $(\bar{f}_1 \bar{f}_2)$, and only $(f_1 f_2)$ contributes to the first diagonal according to [13], [30]. It is similar to that of Werner systems.

Noisy Gates. The above assumes that the gates are noiseless. When they are noisy, the output fidelity of swapping and purification is affected by the accuracy of used gates. Typically, three types of gates are involved: 1-qubit gates, 2-qubit gates, and BSM gates. Formulas including the impact of these three types of gates can be found in [14], [30], [33]. We will use them in evaluations for noisy Werner systems.

C. OSPS Problem and Tree-based Modeling

We now formally introduce the *Optimal Swapping and Purification Scheme* (OSPS) Problem on a quantum path between an SD pair.

Definition 1: **OSPS Problem**: Given a simple quantum path $n_1 \leftrightarrow n_N$ with $N-1$ edges/hops $\{e_1, e_2, ..., e_{N-1}\}$ where the edge e_i connects nodes n_i and n_{i+1} and generates a limited number of entanglements in a time period, how to use swapping and purification operations to create an E2E entanglement between the SD pair nodes of n_1 and n_N so that (1) the fidelity of generated entanglement is larger or equal to a fidelity threshold F^*; (2) the expected number of original link-level entanglements used is minimized.

Swapping and Purification Tree: Given a quantum path, a Swapping Scheme (SS) defines the order in which quantum swaps are performed to establish an end-to-end entanglement along the path. Similar to [24], we can model any SS using a tree structure, called a *Swapping Tree* (ST). By ignoring purification in the SPS shown in Fig. 1, we can model the swapping scheme along the path $n_1 \leftrightarrow n_5$ in both SPS schemes, whose corresponding ST is the same and shown in Fig. 2(a). Similarly, we can model purification schemes using a *Purification Tree* (PT), as shown in Fig. 2(b). It demonstrates a PT over the link e_1. A slight difference is that a PT only involves entanglements on the same two nodes. When both swapping and purification are used along the path, we can model the SPS using a *Swapping and Purification Tree* (SPT), as shown in Fig. 2(c) and Fig. 2(d) which depict Scheme 1 and Scheme 2 in Fig. 1, respectively. It is clear that both ST and PT are special SPTs.

Fidelity and Cost of SPT: For any of these types of trees, we can compute the fidelity and expected cost of any entanglement (i.e., the expected number of entanglements needed) generated on the corresponding node in the tree in a bottom-up manner. It is obvious that the fidelity can be calculated in a (bottom-up) layer-by-layer fashion using the equations defined in Section III-B. We now show that the **expected cost** can also be calculated by a layer-by-layer method in the tree. Note that (1) if all operations never fail, then the cost is simply the number of leaves in the tree (i.e., the number of entanglements used in total); (2) if we consider the success probabilities of swapping or purification operations, we now use a simple example of three-level tree (as shown in Fig. 3) to illustrate that the expected cost at the root (node A), denoted by $\mathbb{E}[c_A]$, can be calculated as follows:

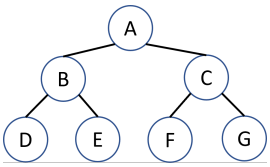

Fig. 3. A 3-level SPT: nodes A, B, C are either swapping or purification, while leaves can be quantum links or sub-SPTs.

$$\mathbb{E}[c_A] = \frac{\mathbb{E}[c_B] + \mathbb{E}[c_C]}{p_A} = \frac{\frac{\mathbb{E}[c_D]+\mathbb{E}[c_E]}{p_B} + \frac{\mathbb{E}[c_F]+\mathbb{E}[c_G]}{p_C}}{p_A}, \quad (7)$$

where c_* and p_* represent the number of entanglements used by the operation on node $*$ and the success probability of the operation on node $*$. The expected cost of a parent node is the ratio between the summation of the cost of its two children (because they are both consumed in the operation) and the successful rate of the operation (i.e., swapping or purification). Due to the space limit, we ignore the formal proof of Eq. (7). By applying this three-layer tree recursively towards the root from the bottom, we can process the whole SPT and calculate the expected cost of this SPT in a layer-by-layer way.

D. Dynamic Programming Solution

Based on the tree modeling, we now introduce a dynamic programming (DP) solution for the dual problem of our OSPS

problem where the cost C (the number of entanglements needed) is given and the optimization goal is to maximize the E2E fidelity. We call such a problem the *optimal fidelity SPS* (OFSPS). Note that the DP solution for OFSPS has the same issue as the early hybrid scheme [13]: the cost needs to be known as input, which makes them not useful when failure is considered. To use DP to solve our OSPS problem, we have to try excessive times (for various costs) to find a proper cost. Moreover, DP cannot solve the OFSPS with operation failures.

We now consider the optimal structure of OFSPS. Let $T(i,j,c)$ denote the optimal fidelity through link e_i to link e_j (inclusive), when the total *expected* budget is c EPR pairs. Then, we have:

$$T(i,j,c) = \max\{\max_{j-i\le k\le c-j+i} P(T(i,j,k), T(i,j,c-k)), \max_{\substack{i<m<j \\ m-i\le k\le c-j+m}} S(T(i,m,k), T(m,j,c-k))\}.$$

This considers the current path fraction as $n_i \leftrightarrow n_j$ with a budget of c. Whenever we get a new entanglement pair (except link-level ones), it is generated from either quantum purification (1st term in the eq.) or swapping (2nd term in the eq.) operations. By exploring all possible path fractions and budget splits, a simple bottom-up DP algorithm can compute the final optimal fidelity $T(1,N,C)$ for OFSPS.

Optimality. Under the assumptions of [10], [15]–[17] (no operation failure, which is actually impossible for purification), this DP algorithm is able to find the optimal solution, as DP algorithms exhaust all possible integer budget splits. However, if failure of operations is considered, the expected cost can be real numbers. As there are infinite possible splits for real numbers, the DP algorithm is not able to try all splits, and thus cannot solve OFSPS (and OSPS).

IV. Analysis of Optimal SPS in Binary Systems

To facilitate better solutions for our OSPS problem, we first analyze the optimal SPS in Binary systems.

SPS Tree Patterns: We first introduce the definitions of two tree patterns: *optimal SPT* (OSPT) and *restricted SPT* (RT).

Definition 2: The *optimal SPT* (OSPT) is an SPT with the least resource cost of the root node, while the root fidelity is no less than a given requirement F^*.

Obviously, the OSPT describes the optimal solution of OSPS.

Definition 3: A *restricted SPT* (RT) is an SPT in which there is no swapping node below a purification node on any path from the root to a leaf.

In an RT, no purification should happen on any pairs generated after one or more swappings. All entanglements participating in any purification either come from (i) entanglement generation on optical links, or (ii) previous purification.

Main Theorem on Optimal Tree Pattern: We prove that any OSPT in Binary systems must be an RT.

Theorem 1: In Binary systems, when $F^* \in (0.5, 1)$, any OSPT of the OSPS problem must be an RT.

Proof: We prove this by contradiction. Assume that there exists an OSPT that is not an RT. Then we show that there exists a transformation that can transform this OSPT into an RT while increasing its root fidelity and decreasing its cost. This is done by recursively transforming subtrees of this OSPT to RTs in a bottom-up way. Finally, the whole OSPT is transformed into an RT which has higher fidelity and less cost than the OSPT, leading to the contradiction.

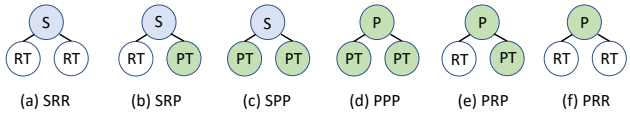

Fig. 4. Six possible SPS tree patterns. Here, the pattern is named by 'the root'-'left subtree'-'right subtree', where 'the root' can be swapping (S) or purification (P), and 'subtree' can be either a pure PT (P) or an RT (R).

Now we show how to conduct such transformations. When the subtrees are limited to RT and PT, there are six distinct internal node patterns, as shown in Fig. 4. We use three letters (for 'the root'-'left subtree'-'right subtree') to name these patterns. These six patterns are universal because (1) there are $2^3 = 8$ trees in total, but exchanging left and right subtrees keeps the tree identical, so only 6 out of 8 are left; (2) RT includes PT, but we assume that any RT in those patterns are not PT. That is because, in those cases, the pattern degrades to one of the others. For example, if one of the RTs in SRR is a PT and the other is not, then the SRR is actually an SRP.

First, for four patterns (SRR, SRP, SPP, and PPP), the overall tree is already an RT, so we only need to handle the other two cases (PRP and PRR). Second, in PRP (Fig. 4(e)), the right child is a pure PT over one link. As the left RT child can perform the purification operation with this right PT, they must share the same end nodes (i.e., on the same two adjacent routers). That is, this RT must be either the leaf that the PT purifies or another PT over this leaf. Note that a potential counter-example is when the RT forms a ring with the leaf: the RT is not a PT but still has the same ends as the leaf's. But this is impossible because SPT is defined on a non-cyclic simple path. Thus, this PRP is actually a PT without any swapping, thus it is a PPP, an RT too. Last, for PRR (Fig. 4(f)), we want to prove that it can be transformed into an SRR with better fidelity and cost. In a Binary system, we can formally prove this as Lemma 2. Generally, Lemma 2 tells us that we can lift the two 'S' nodes in PRR one level upwards, without violating its optimality.

Till now, we can transform the above 6 patterns into RT without decreasing the fidelity or increasing the cost. Now, we explain how to transform any SPT into an RT. For a non-RT SPT, we can process it in a bottom-up way: we find the shallowest 'S' node whose parent is 'P' (so a PRR). It must exist otherwise the SPT is an RT. And the children of this 'S' must be RT as it is the shallowest 'S'. We can lift the 'S' nodes to transform the subtree into an RT by applying Lemma 2. By repeating this transformation, we can concentrate all 'S' nodes towards the root. Finally, we can transform any SPT into an RT with increased fidelity and decreased cost. This contradicts the fact that the OSPT is optimal. ■

Lemma 2: In Binary systems, when all nodes' fidelity $f \in (0.5, 1)$, any PRR can be transformed into SRR with increased

fidelity and reduced cost.

Proof: Due to space limitations, we cannot include the detailed proof, instead, we explain its basic idea here. We can quantify the fidelity and cost before and after the transformation via our layer-by-layer processing. Then, we get a set of two inequalities: one states that the cost is smaller after the transformation; the other states that the fidelity is higher after the transformation. We can find that the necessary and sufficient condition for both inequalities is that the fidelity of children in $(0.5, 1)$, which is reasonably true in Binary systems[1]. ■

Discussions: From Theorem 1, we can draw two main conclusions for Binary systems. First, to search for OSPS, we no longer need to consider all SPSes (i.e. all SPTs) but only focus on those of RTs. This greatly reduces the complexity of its search. Second, for the design of protocols and devices (e.g., routers), we may directly integrate the purification at the link level, which separates the swapping and purification. The protocol may send a requirement for link-level fidelity, then the routers of a link collaborate locally to generate such entanglements while the protocol can arrange the swapping. Such a design may greatly reduce the complexity of network-wide fidelity-aware protocols (compared with hybrid SPS).

Besides, because RT is an ST of PT (take the root nodes of PTs as leaves of the ST), we can propose an intuitive solution framework (for the OSPS problem) consisting of three stages: (i) PT shape search; (ii) ST shape search; (iii) sacrificial pair allocation. Existing works [10], [11], [20] do not do shape search because S_b, S_w, P_b (i.e., Eq. (3), Eq. (4), Eq. (5)) are all associative. That is, the orders of (i) swapping in Binary systems, (ii) purification in Binary systems, and (iii) swapping in Werner systems do not affect the final fidelity of an SPS. But *when the failure of operations occurs, the order now matters in both systems, as the expected cost is not associative anymore*. Theorem 1 also implies that combining the optimal solution for each stage can lead to the optimal solution overall. However, finding the optimal PT and ST shapes is still challenging. Existing works [10], [11] both somehow follow this 3-stage framework. However, since Theorem 1 is not true for Werner systems, such a framework may not even be able to generate a feasible solution. We will confirm that [10], [11] are indeed empirically infeasible in the evaluation section.

V. Proposed Branching Tree Algorithm

Based on our previous analysis, we are able to tell the limits of the current solution and now propose a new efficient tree-based SPS algorithm (TREE) that works in both considered scenarios (i.e., *Binary systems* and *Werner systems*).

Overall Framework: We first introduce the main workflow of our proposed algorithm. The basic idea is, with the help of the tree structure, we can repeat the following loop until the E2E fidelity is high enough: (i) find a proper node to purify; (ii) purify the node; (iii) update the tree. The workflow is shown in Algorithm 1. First, BUILD-ST constructs an ST of the router chain without any purification. Then, the loop starts, and Fig. 5 shows an example of flow within a single loop.

[1]The fidelity of any node in a SPT in Binary systems should always be in $(0.5, 1)$. Since if a node has $f \leq 0.5$, both swapping and purification will propagate this low fidelity towards the root to make the root's fidelity no greater than 0.5 which is useless in a Binary system.

Algorithm 1 BRANCHING TREE SPS (TREE)

Input: link fidelity array F, fidelity threshold F^*.
Output: final fidelity f, (root of) SPT t.

```
f, t = BUILD-ST(F)
while f < F* do
    GRAD(t)  ▷ forward gradient from root to each node
    CALC-EFFICIENCY(t)
    n = FIND-MAX-EFFICIENCY(t) ▷ find the most eff. n
    n = PURIFY(n)              ▷ purify and update n
    f, t = BACKWARD(n)         ▷ update nodes backwards
return f, t
```

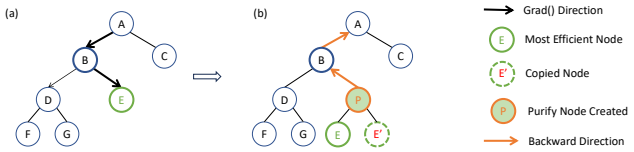

Fig. 5. Control flow of TREE in one single loop: (a) shows gradient calculation and node finding prior to purification; (b) shows the purification followed by ancestors updating.

1) GRAD() calculates the gradients of each node w.r.t. the root. The gradients consist of two parts: (i) gradient of fidelity G_f, (ii) gradient of cost G_c. They are used to estimate how many purification impacts the root node, in terms of fidelity and cost increase.
2) CALC-EFFICIENCY() estimates the efficiency of purifying each node, i.e. (increased fidelity)/(increased cost).
3) We find the node with the highest efficiency and conduct purification at that node.
4) Finally, as the purified node (with its subtree) is replaced by a new node, we call BACKWARD() to update this information to all its ancestors till root.

One of the advantages of this gradient-based design is its efficiency. By utilizing gradients, we can estimate the impact of purifying any node locally: we do not need to go backward (to the root) to know the impact on the root node. Then, because all functions inside the loop are $O(M)$ (where M is the number of nodes in the tree), we can do one purification in $O(M)$ time. Otherwise, without the gradients, we have to backtrack to root for every node, resulting in $O(M^2)$.

Key Steps: we now provide more details of each key step.

BUILD-ST(). It simply creates an ST for the given links in the quantum path. The shape of ST is a factor in the performance of this algorithm, but again, we leave the shape search for ST as future work. Currently, we simply build a balanced tree, but any other swapping tree method can be used.

GRAD(). Note that all swapping/purification functions, both for fidelity and cost (probability), are (compositionally) differentiable. We can compute the gradient of any node w.r.t. to the root, according to the chain rule (for calculating derivatives).

It is similar to the computational graph design (auto-grad) in machine learning frameworks (like PyTorch, TensorFlow, etc).

Each node should maintain two gradients: *the gradient of fidelity* ($G_f(*)$) and *the gradient of cost* ($G_c(*)$), where the $*$ is the corresponding node. $G_f(*)$ is relatively easy to compute because a node's fidelity is only determined by the fidelity of its children. However, $G_c(*)$ is determined by both the fidelity and the cost of its children for the purification operation. Therefore, $G_c(*)$ for a purification node (denoted by $G_c^P(*)$) is actually a vector of two partial gradients, i.e., $G_c^P(*) = (G_{c,f}^P(*), G_{c,c}^P(*))$. For the swapping operation, the cost gradient $G_c^S(*)$ is only determined by the cost of its children, so we set $G_{c,f}^S(*) = 0$. Thus, for either swapping or purification, we have three gradients to calculate, resulting in six gradients in total.

Suppose that we are calculating the gradients of node E in Fig. 5 (when the algorithm reaches its parent node B), we use

$$G_f^S(E) = \frac{\partial S(f_D, f_E)}{\partial f_E} \cdot G_f(B), \tag{8}$$

$$G_{c,c}^S(E) = \frac{\partial S(c_D, c_E)}{\partial c_E} \cdot G_{c,c}(B) = \frac{G_{c,c}(B)}{Pr\{S\}}, \tag{9}$$

$$G_{c,f}^S(E) = 0,$$

$$G_f^P(E) = \frac{\partial P(f_D, f_E)}{\partial f_E} \cdot G_f(B), \tag{10}$$

$$G_{c,c}^P(E) = \frac{\partial P(f_D, f_E, c_D, c_E)}{\partial c_E} \cdot G_{c,c}(B),$$

$$G_{c,f}^P(E) = \frac{\partial P(f_D, f_E, c_D, c_E)}{\partial f_E} \cdot G_{c,f}(B). \tag{11}$$

Based on the actual operation (swapping or purification) of E's parent node B, we use either Eq. (8, 9) or Eq. (10,11). Note $G_f(B)$ is the fidelity gradient of parent node B. When B is not the root, $G_f(B)$ is already calculated when the algorithm reaches B's parent node. If B is the root, its gradient is set to 1. For Eq. (9), the cost of swapping operations is calculated by Eq. (7), thus $\frac{\partial S(c_D,c_E)}{\partial c_E} = \frac{1}{p_B} = \frac{1}{Pr\{S\}}$.

When estimating the cost increase at the root A (caused by this purification at E), $\Delta_c(A) = (\Delta_f(E), \Delta_c(E)) \times (G_{c,f}(E), G_{c,c}(E))$, where $\Delta_f(E)$ and $\Delta_c(E)$ are the fidelity and cost increase after purifying node E, both of which can be locally computed. With the help of gradients, we are able to estimate the impact of an operation on the root, without tracing back to the root.

According to the chain rule, we can repeat such differentiation for both functions from the root to all leaves. Then, for CALC-EFFICIENCY(), the efficiency of node E is

$$\delta(E) = \frac{\Delta_f(A)}{\Delta_c(A)} = \frac{\Delta_f(E) \times G_f(E)}{(\Delta_f(E), \Delta_c(E)) \times (G_{c,f}(E), G_{c,c}(E))}. \tag{12}$$

PURIFY(). To purify a node, for example, E, we need to (i) make a copy of this node, say E', (ii) create a new purification node P whose children are E and E', (iii) replace the node E by P in the tree.

TABLE I
DEVICE PARAMETERS FOR WERNER AND BINARY SYSTEMS.

Setting	α_1	α_2	η	Pr$\{S_w\}$	Pr$\{S_b\}$
P	1	1	1	1	1
H	$1-10^{-5}$	$1-10^{-5}$	$1-10^{-4}$	0.75	0.75
L	$1-10^{-3}$	$1-10^{-3}$	$1-10^{-2}$	0.5	0.5

P: perfect (no error/noise); H/L: high/low accuracy/reliability.

TABLE II
NETWORK DESCRIPTION.

Scale	SD #	Topology	$\|V\|$	$\|E\|$
Small	13	$AT\&T$	25	104
Medium	25	$G(50, 0.1)$	50	121
Large	50	$P(100, 2)$	100	196

Finally, BACKWARD(). Suppose we have just performed PURIFY for a node (or a subtree), now we need to update all ancestors of the new node P. The red arrows in Fig. 5 show the trace of BACKWARD(). We backtrack from node P until the root. Whenever reaching a new ancestor, we re-calculate its fidelity and cost using the new information from its children.

In the next round, if we hope to do another purification, GRAD() and CALC-EFFICIENCY() will update the gradients and efficiencies of all nodes. The loop is repeated until the E2E fidelity reaches the threshold.

Analysis: An implicit property of the TREE method is that its output SPT is always an RT in Binary systems. This property is favorable because, though not all RTs are optimal, they include optimal trees in Binary systems (by Theorem 1).

Theorem 3: For Binary systems ($f \in (0.5, 1)$), TREE method never purifies a SWAP node and generates an RT.

Proof: Note that if swapping nodes are never purified, we cannot get a non-trivial PRR pattern in the tree so it is an RT; if the tree is not an RT, there must be at least one non-trivial PRR, which implies that a swapping node is purified. Due to space limitations, we only briefly introduce how to prove that the swapping node cannot be more efficient than its two children at the same time. We can instantiate Eq. (12) for a swapping node and its two children. Then, we build a set of two inequalities: one states that the parent's efficiency is greater than the left child's; the other states that the parent's efficiency is greater than the right child's. Solving the set of inequalities, we can see that it requires $(f_l - \frac{1}{2})(f_r - \frac{1}{2}) > \frac{1}{4}$ or $(f_l - \frac{1}{2})(f_r - \frac{1}{2}) < -\frac{3}{4}$, where f_l/f_r is the fidelity of the left/right child. Since both f_l and f_r are in $(0.5, 1)$, the inequality set can never be satisfied. That is, the efficiency of any swapping node cannot be greater than its two children at the same time, so the TREE algorithm never purifies a swapping node (but its children or deeper descendants). ■

VI. EVALUATIONS

To evaluate the proposed method and the baselines, we have conducted experiments for both Binary and Werner systems under different operations (gates) noise levels.

A. Experiment Setup

Default Network Settings. Each SD pair requires no more than 10 entanglements. Node memory is 100 and link capacity is 50 (by [34]). For Binary systems, link fidelity is randomly

drawn from $(0.7, 0.95)$ based on [10]. For Werner systems, we set it drawn from $(0.95, 1)$, since it is harder to maintain connections in Werner systems. The number of candidate paths between any SD pair is set to 5. The accuracy (or success probability) of quantum gates is specified in Table I, set based on current/near future achievable devices [27]–[29], [35], [36]. In the table, α_1, α_2, η represent the fidelity of 1-qubit, 2-qubit, and BSM gates used for noisy Werner systems. For network topology, we use three types of network size summarized in Table II. $AT\&T$ is a real topology from [37], $G(n, p)$ and $P(n, m)$ are Erdos-Renyi graphs with parameters n/p and preferential attachment model with parameters n/m, respectively. Those networks/models have been used in [9].

Baselines. We compared five different SPS methods (three existing methods and two of our proposed methods), which can be grouped into two groups.

Group 1 includes methods designed for OSPS, i.e., accepting the E2E fidelity threshold as input and minimizing the used entanglements to reach the fidelity threshold.

1) **TREE**: our proposed branching tree method in Section V.
2) **GRDY**: a greedy algorithm [11] that greedily selects the link with the highest final fidelity increase.
3) **EPP**: an entanglement path preparation method [10] that greedily finds the link with the largest fidelity gradient.

Group 2 contains methods for OFSPS, i.e., needs a predetermined budget and aims to find the highest achievable fidelity. Note that the real used cost may be higher than the budget (because these methods do not consider failures), and some may not be able to generate a feasible solution for OSPS.

4) **DP-x**: our proposed DP solution in Section III-D with a input budget of x times the cost given by TREE method.
5) **NESTED**: the nested (hybrid) purification method from [13], which is based on a fixed SPS and requires the total budget should be $(ly)^z$, where l is the fragment length, y is the budget for each link per level, and z is the nest level. Here, we decide the best l, y, and z according to the path length and budget from TREE method. The calculated y can be fractional, so we use both its floor and ceiling (denoted as NESTED-F and NESTED-C).

Note that we do not include the methods from [17] because they do not consider operation failures and it is non-trivial to calculate their methods' real expected cost under failures.

Performance Metrics. To evaluate the proposed methods and baselines, we focus on their competency in providing high-fidelity entanglements. We compare their (i) cost (number of sacrificial entanglements) required to reach specific fidelity on a single path; (ii) impact on network-wide throughput under fidelity requirements. For a fair comparison in the network-wide throughput, we use the entanglement path selection method from [10] as the network scheduler for all baselines.

B. Evaluation Results

We first report the results on path efficiency in both Binary and Werner systems, then show their network throughput performances. Results are the average of 20 separate runs.

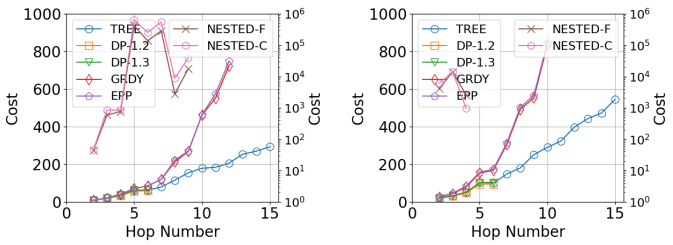

(a) $F^* = 0.9$ (b) $F^* = 0.99$

Fig. 6. Path efficiency (cost) of all methods with different F^* in Binary systems (device level H, i.e., $\Pr\{S_b\} = 0.75$).

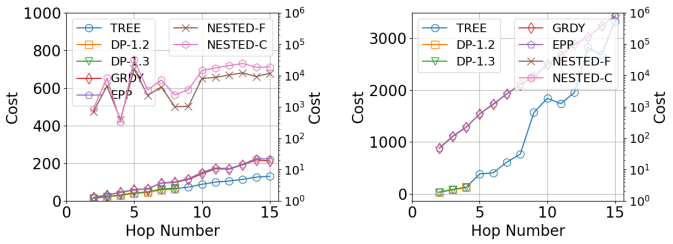

(a) $\Pr\{S_b\} = 1.0$ (b) $\Pr\{S_b\} = 0.5$

Fig. 7. Path efficiency (cost) of all methods under different device reliability levels in Binary systems ($F^* = 0.99$).

1) Path Efficiency in Binary System: We now investigate how well the algorithms can establish one single E2E entanglement on one single path. Fig. 6 provides the results of all methods in the Binary system under different fidelity thresholds. NESTED methods (and sometimes other methods) typically use significantly more entanglements compared to TREE and DP, so they are drawn in a logarithmic scale (right y-axis). For clarity, we limit the right y-axis to 10^6, so NESTED is sometimes cut-off as its cost is too large on long paths. We can observe the following. First, to generate E2E entanglement on a longer path, more entanglements (i.e., larger cost) are needed. Second, for higher fidelity requirement F^*, a larger cost is needed. Third, for all cases (different F^*), our method TREE uses the least number of sacrificial entanglements (except the tuned DP methods, explained later), which implies it can achieve higher network-wide throughput when employed by a network-wide scheduler. Last, when F^* is closer to 1, the more entanglement resources our method saves compared with GRDY, EPP and NESTED. Although GRDY and EPP follow the PS strategy, they do not perform well since they simply use sequential swapping and purification. While TREE is agnostic to the SPS schemes, it automatically follows the PS, and conducts shape search for PTs. NESTED fluctuates heavily because it performs much better at certain path length that can be written as exponents, such as 4 and 8.

Fig. 7 plus Fig. 6(b) shows the results with different reliability levels when $F^* = 0.99$. We have three reliability ($\Pr\{S_b\}$) levels (P, H, L) for Binary systems as shown in Table I. Obviously, lower reliability leads to larger costs. Fig. 8(a) also reports the achieved E2E fidelity when $F^* = 0.99$ and device level is H. As shown in Figs. 6, 7, 8(a), NESTED methods consume much more entanglements than TREE does, while

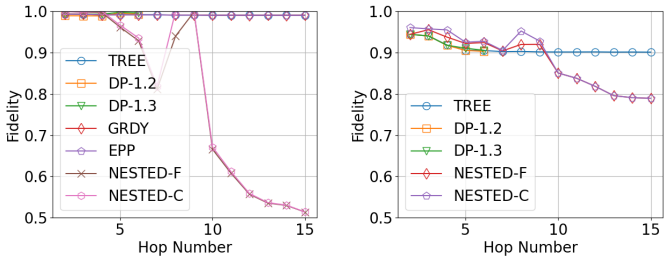

(a) Binary, $F^* = 0.99$ (b) Werner, $F^* = 0.9$

Fig. 8. Achieved E2E fidelity of different methods in Binary and Werner systems when the device level is H.

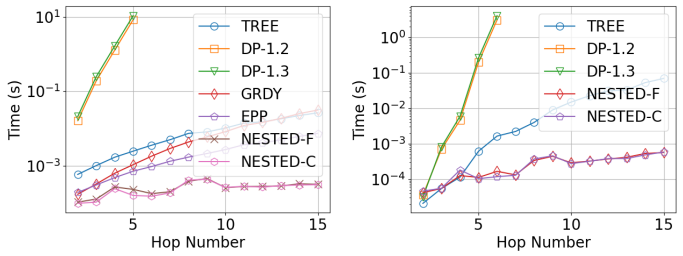

(a) Binary, $F^* = 0.99$ (b) Werner, $F^* = 0.9$

Fig. 9. Running time of different methods in Binary and Werner systems when the device level is H.

still cannot generate comparable E2E fidelity in most cases. Again, it may perform well at certain path lengths (like 8 and 9) due to its design, but significantly worse at other lengths.

Fig. 9(a) reports the running time of all methods. Obviously, a longer path or higher F^* leads to longer running time. NESTED is always the most efficient one as it uses a predetermined SPS. TREE, GRDY, and EPP all use greedy strategies, so they have similar running time performance. We pick DP-1.2/1.3 to represent the DP method because (i) they cost slightly fewer or more entanglements compared with TREE (Fig. 6 and Fig. 7); (ii) their achieved E2E fidelity is slightly lower or higher than TREE's (Fig. 8(a)). Not surprisingly, DP is inefficient as it has to try all budget splits, which can be very large when the path is long. The running time of DP increases drastically as the path length increases, so we do not test it on long paths here.

In summary, in Binary systems, NESTED performs the worst in terms of fidelity and cost. Recall that Theorem 1 shows that the OSPT in Binary systems should arrange purification before swapping. But NESTED clearly disobeys such a structure. The other methods follow the PS structure, resulting in better efficiency compared to NESTED.

2) Path Efficiency in Werner System: We also compare TREE with Group 2 methods (DP and NESTED) in terms of fidelity, cost, and running time in Werner systems. We do not consider GRDY and EPP here, since both do not work in Werner systems. For example, both cannot purify a simple 2-hop path: set links fidelity and threshold F^* to 0.95, the outer loops in GRDY/EPP cannot stop.

Figs. 10, Fig. 8(b) and Fig. 9(b) show the results in Werner systems with highly reliable devices. We can draw similar conclusions regarding all methods similar to that in Binary systems. DP-1.3 and DP-1.4 consume similar costs and

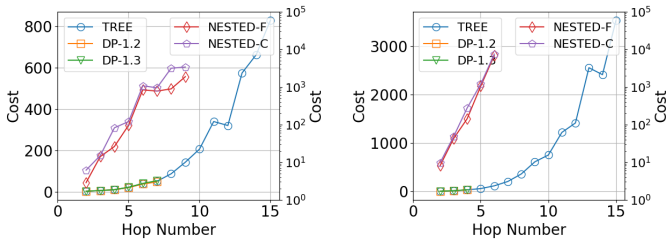

(a) $F^* = 0.9$ (b) Werner, $F^* = 0.95$

Fig. 10. Path efficiency of Group 2 methods under different F^* in Werner systems when the device level is H.

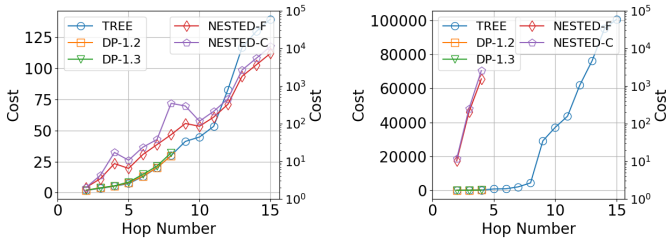

(a) device level of P (b) device level of L

Fig. 11. Path efficiency of Group 2 methods under different device reliability levels in Werner systems ($F^* = 0.9$).

achieve similar fidelity to TREE's, but still become extremely inefficient in terms of running time when the path is long. NESTED behaves similarly in Werner systems compared with Binary ones: (i) it typically consumes much more entanglements while does not achieve comparable E2E fidelity compared with TREE; (ii) it performs better when the path length is an exponent; (iii) it usually finishes quickly. Overall, our proposed method TREE still performs best in Werner systems with highly reliable devices.

We also consider Werner systems with devices of different reliability levels in Fig. 11 when $F^* = 0.9$. Results are similar to those in the highly reliable Werner system (Fig. 10(a)). The difference is that all methods need more entanglements to achieve the same fidelity when the system is noisy.

3) Network Throughput in Binary/Werner Systems: Finally, we evaluate the network-wide throughput when the proposed TREE and baselines (if work in the corresponding scenarios) are used for solving the candidate paths in a network scheduler [10] in both Binary and Werner systems. We consider three sizes of networks, defined in Table II. We do not include DP in this evaluation because it requires too long time for long paths even in a small network and if such paths are selected the scheduler will be stuck by DP. GRDY and EPP are not tested for Werner systems as they do not work there.

Results are reported in Fig. 12. Obviously, in a smaller network (so less demands), the throughput of all methods is smaller. More importantly, in all cases, our method TREE achieves the highest throughput among all methods. We also perform tests over different F^* and different noise levels (P, H and L), but due to space limitations, we ignore reporting the results here. Among the different noise levels, a lower noise level always leads to higher throughput.

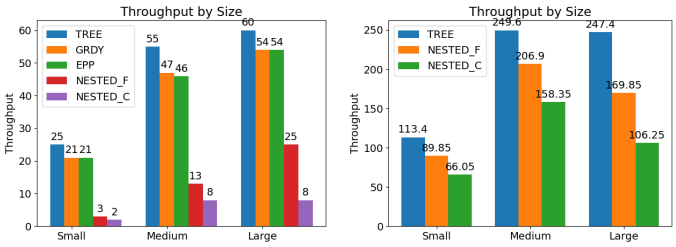

(a) Binary, $F^* = 0.99$ (b) Werner, $F^* = 0.9$

Fig. 12. Network throughput of all methods for networks with different sizes when the device level is H.

VII. Conclusion

We studied the joint swapping and purification scheme to generate the required E2E fidelity for an SD pair while the consumed entanglements are minimized. We considered more general assumptions (both Binary and Werner systems with possible failures of swapping/purification operations). By leveraging tree-based modeling, we proved that the optimal SPS in Binary systems is a PS strategy where purification is before swapping. We then proposed a tree-based solution that first time works for the SPS problem in both Binary and Werner systems. We confirmed nice performances of the proposed method compared with existing solutions in both Binary and Werner systems via extensive simulations.

References

[1] R. Van Meter, *Quantum networking*. John Wiley & Sons, 2014.

[2] A. Dahlberg, M. Skrzypczyk, T. Coopmans, L. Wubben, F. Rozpędek, M. Pompili, A. Stolk, P. Pawełczak, R. Knegjens, J. de Oliveira Filho *et al.*, "A link layer protocol for quantum networks," in *Proc. of ACM SIGCOMM*, 2019, pp. 159–173.

[3] Y. Wang, A. N. Craddock, R. Sekelsky, M. Flament, and M. Namazi, "Field-deployable quantum memory for quantum networking," *Physical Review Applied*, vol. 18, no. 4, p. 044058, 2022.

[4] J. Liu, L. Fan, Y. Guo, Z. Han, and Y. Wang, "Co-design of network topology and qubit allocation for distributed quantum computing," in *Proc. of IEEE Int'l Conf on Quantum Communications, Networking, and Computing (QCNC)*, 2025.

[5] X. Wei, L. Fan, Y. Guo, Z. Han, and Y. Wang, "Optimizing satellite-based entanglement distribution in quantum networks via quantum-assisted approaches," in *Proc. of IEEE Int'l Conf on Quantum Communications, Networking, and Computing (QCNC)*, 2024.

[6] X. Wei, J. Liu, L. Fan, Y. Guo, Z. Han, and Y. Wang, "Optimal entanglement distribution problem in satellite-based quantum networks," *IEEE Network*, vol. 39, no. 1, pp. 97-103, 2025.

[7] J. Liu, X. Liu, X. Wei, and Y. Wang, "Topology design with resource allocation and entanglement distribution for quantum networks," in *Proc. of IEEE Int'l Conf. on Sensing, Commun., & Net. (SECON)*, 2024.

[8] X. Wei, L. Fan, et al., "Entanglement from sky: Optimizing satellite-based entanglement distribution for quantum networks," *IEEE/ACM Trans. on Networking*, vol. 32, no. 6, p. 5295-5309, 2024.

[9] S. Pouryousef, N. K. Panigrahy, and D. Towsley, "A quantum overlay network for efficient entanglement distribution," *arXiv preprint arXiv:2212.01694*, 2022.

[10] Y. Zhao, G. Zhao, and C. Qiao, "E2E fidelity aware routing and purification for throughput maximization in quantum networks," in *IEEE INFOCOM 2022-IEEE Conference on Computer Communications*. IEEE, 2022, pp. 480–489.

[11] J. Li, M. Wang, K. Xue, R. Li, N. Yu, Q. Sun, and J. Lu, "Fidelity-guaranteed entanglement routing in quantum networks," *IEEE Transactions on Communications*, vol. 70, no. 10, pp. 6748–6763, 2022.

[12] W. Dai, T. Peng, and M. Z. Win, "Optimal remote entanglement distribution," *IEEE Journal on Selected Areas in Communications*, vol. 38, no. 3, pp. 540–556, 2020.

[13] W. Dür, H.-J. Briegel, et al., "Quantum repeaters based on entanglement purification," *Physical Review A*, vol. 59, no. 1, p. 169, 1999.

[14] N. K. Panigrahy, T. Vasantam, D. Towsley, and L. Tassiulas, "On the capacity region of a quantum switch with entanglement purification," *arXiv preprint arXiv:2212.01463*, 2022.

[15] L. Chen and Z. Jia, "On optimum entanglement purification scheduling in quantum networks," *IEEE Journal on Selected Areas in Communications*, vol. 42, no. 7, pp. 1779–1792, 2024.

[16] Z. Jia and L. Chen, "From entanglement purification scheduling to fidelity-constrained entanglement routing," in *2024 IEEE 32nd International Conference on Network Protocols (ICNP)*, 2024.

[17] Z. Jia and L. Chen, "From entanglement purification scheduling to fidelity-constrained multi-flow routing," *arXiv preprint arXiv:2408.08243*, 2024.

[18] A. Farahbakhsh and C. Feng, "Opportunistic routing in quantum networks," in *IEEE INFOCOM 2022-IEEE Conference on Computer Communications*. IEEE, 2022, pp. 490–499.

[19] Y. Zeng, J. Zhang, J. Liu, Z. Liu, and Y. Yang, "Multi-entanglement routing design over quantum networks," in *IEEE INFOCOM 2022-IEEE Conference on Computer Communications*. IEEE, 2022, pp. 510–519.

[20] H. Gu, Z. Li, R. Yu, X. Wang, F. Zhou, and J. Liu, "FENDI: High-fidelity entanglement distribution in the quantum internet," *arXiv preprint arXiv:2301.08269*, 2023.

[21] L. Yang, Y. Zhao, H. Xu, and C. Qiao, "Online entanglement routing in quantum networks," in *2022 IEEE/ACM 30th International Symposium on Quality of Service (IWQoS)*. IEEE, 2022, pp. 1–10.

[22] M. Victora, S. Tserkis, S. Krastanov, A. S. de la Cerda, S. Willis, and P. Narang, "Entanglement purification on quantum networks," *Phys. Rev. Res.*, vol. 5, p. 033171, Sep 2023. [Online]. Available: https://link.aps.org/doi/10.1103/PhysRevResearch.5.033171

[23] L. Jiang, J. M. Taylor, N. Khaneja, and M. D. Lukin, "Optimal approach to quantum communication using dynamic programming," *Proc. of the National Academy of Sci.*, vol. 104, no. 44, pp. 17 291–17 296, 2007.

[24] M. Ghaderibaneh, C. Zhan, H. Gupta, and C. Ramakrishnan, "Efficient quantum network communication using optimized entanglement swapping trees," *IEEE Trans on Quantum Eng.*, vol. 3, pp. 1–20, 2022.

[25] A. Chang and G. Xue, "Order matters: On the impact of swapping order on an entanglement path in a quantum network," in *IEEE INFOCOM 2022 Workshops (INFOCOM WKSHPS)*. IEEE, 2022, pp. 1–6.

[26] R. Van Meter, *Quantum networking*. John Wiley & Sons, 2014.

[27] M. J. Bayerbach, S. E. D'Aurelio, P. van Loock, and S. Barz, "Bell-state measurement exceeding 50% success probability with linear optics," *Science Advances*, vol. 9, no. 32, p. eadf4080, 2023.

[28] F. Ewert and P. van Loock, "3/4-efficient bell measurement with passive linear optics and unentangled ancillae," *Physical review letters*, vol. 113, no. 14, p. 140403, 2014.

[29] A. Kamimaki, K. Wakamatsu, K. Mikata, Y. Sekiguchi, and H. Kosaka, "Deterministic bell state measurement with a single quantum memory," *npj Quantum Information*, vol. 9, no. 1, p. 101, 2023.

[30] D. Deutsch, A. Ekert, R. Jozsa, et al., "Quantum privacy amplification and the security of quantum cryptography over noisy channels," *Physical review letters*, vol. 77, no. 13, p. 2818, 1996.

[31] C. H. Bennett, G. Brassard, S. Popescu, et al., "Purification of noisy entanglement and faithful teleportation via noisy channels," *Physical review letters*, vol. 76, no. 5, p. 722, 1996.

[32] C. H. Bennett, D. P. DiVincenzo, J. A. Smolin, and W. K. Wootters, "Mixed-state entanglement and quantum error correction," *Physical Review A*, vol. 54, no. 5, p. 3824, 1996.

[33] A. Zang, X. Chen, et al., "Entanglement distribution in quantum repeater with purification and optimized buffer time," *arXiv preprint arXiv:2305.14573*, 2023.

[34] Y. Lee, E. Bersin, A. Dahlberg, S. Wehner, and D. Englund, "A quantum router architecture for high-fidelity entanglement flows in quantum networks," *npj Quantum Information*, vol. 8, no. 1, p. 75, 2022.

[35] X. Rong, J. Geng, F. Shi, Y. Liu, K. Xu, W. Ma, F. Kong, Z. Jiang, Y. Wu, and J. Du, "Experimental fault-tolerant universal quantum gates with solid-state spins under ambient conditions," *Nature communications*, vol. 6, no. 1, p. 8748, 2015.

[36] R. Reyes, T. Nakazato, N. Imaike, K. Matsuda, K. Tsurumoto, Y. Sekiguchi, and H. Kosaka, "Complete bell state measurement of diamond nuclear spins under a complete spatial symmetry at zero magnetic field," *Applied Physics Letters*, vol. 120, no. 19, 2022.

[37] "Traffic engineering applying value at risk," https://github.com/manyaghobadi/teavar,.